

M²UNet: MetaFormer Multi-scale Upsampling Network for Polyp Segmentation

Quoc-Huy Trinh[✉], Nhat-Tan Bui[✉], Trong-Hieu Nguyen-Mau[✉],
Minh-Van Nguyen[✉], Hai-Minh Phan[✉], Minh-Triet Tran[✉], Hai-Dang Nguyen[✉]

*Faculty of Information Technology, Software Engineering Laboratory,
International Training and Education Center, and John von Neumann Institute
University of Science, VNU-HCM*

Vietnam National University, Ho Chi Minh City, Vietnam

20120013@student.hcmus.edu.vn, 1859043@itec.hcmus.edu.vn, 20120081@student.hcmus.edu.vn,
nmvan20@clc.fitus.edu.vn, phminh22@clc.fitus.edu.vn, tmtriet@fit.hcmus.edu.vn, nhdang@selab.hcmus.edu.vn

Abstract—Polyp segmentation has recently garnered significant attention, and multiple methods have been formulated to achieve commendable outcomes. However, these techniques often confront difficulty when working with the complex polyp foreground and their surrounding regions because of the nature of convolution operation. Besides, most existing methods forget to exploit the potential information from multiple decoder stages. To address this challenge, we suggest combining MetaFormer, introduced as a baseline for integrating CNN and Transformer, with UNet framework and incorporating our Multi-scale Upsampling block (MU). This simple module makes it possible to combine multi-level information by exploring multiple receptive field paths of the shallow decoder stage and then adding with the higher stage to aggregate better feature representation, which is essential in medical image segmentation. Taken all together, we propose MetaFormer Multi-scale Upsampling Network (M²UNet) for the polyp segmentation task. Extensive experiments on five benchmark datasets demonstrate that our method achieved competitive performance compared with several previous methods.

Index Terms—MetaFormer, UNet, Polyp Segmentation

I. INTRODUCTION

Colorectal cancer poses a significant threat to human health and society, making it a substantial health concern. Polyps, which are abnormal growths in the colon or rectum, have the potential to develop into cancerous tumors over time. Early detection of polyps plays a vital role in preventive healthcare, as it can greatly improve the prognosis and treatment effectiveness for individuals with colorectal cancer [1].

In recent years, early diagnosis has emerged as a critical factor in treating and preventing colorectal cancer, particularly in polyp detection. However, the accuracy of early diagnosis is constrained by various external factors, as highlighted in [2]. Consequently, polyp segmentation has become an integral component of the diagnostic process.

Deep Learning approaches have gained prominence in polyp image segmentation, with methods such as UNet [3], UNet++ [4], PraNet [5], MSNet [6], and PEFNet [7], demonstrating competitive performance in state-of-the-art results. While Convolutional Neural Network (CNN) models excel in capturing local information, they face challenges in comprehensively representing the overall shape of polyp objects, which is

crucial for precise segmentation. This limitation significantly contributes to missed segment areas, which are essential outputs in segmentation tasks. Moreover, existing methods mainly concentrate on improving the feature representations of the encoder and skip connection but forget to consider the decoder.

In this paper, we propose the MetaFormer Multi-scale Upsampling Network (M²UNet) that combines MetaFormer [8] with UNet [3] and a Multi-scale Upsampling block (MU). The MetaFormer framework [8] facilitates incorporating both local and global information by employing convolution-based downsampling to capture local features while utilizing a Transformer encoder to capture global features in subsequent stages.

Besides, our MU module enhances the ability to capture multi-level information between multiple decoder stages, further ameliorating the segmentation results of the entire architecture. The MU module specifically employs two receptive field paths to exploit the information of feature maps in different aspects. The output features of MU are cumulative with the features of the decoder layer one stage away, which helps the model extract comprehensive information from different levels of the decoder. Our proposed method shows competitive results on various datasets, demonstrating our model’s ability against the weaknesses of existing approaches.

To summarize, our contributions are threefold:

- We propose the MetaFormer Multi-scale Upsampling Network, termed as M²UNet, combining MetaFormer with UNet for improving the local and global contextual representations of the polyp objects.
- We introduce a Multi-scale Upsampling block (MU) for enhancing the representation ability of different levels of decoder features.
- We demonstrate the effectiveness of our method on five benchmark datasets: Kvasir-SEG [9], CVC-ClinicDB [10], CVC-ColonDB [11], ETIS [12] and CVC-300 [13].

The content of this paper is organized as follows. In Section II, we briefly review existing methods related to this research. Then we propose our methods in Section III. Experiments and discussion are in Section IV. Finally, we present the conclusion in Section V.

II. RELATED WORK

UNet [3] sets a new precedent as it was the first model to integrate skip connections in the encoder-decoder architecture, specifically for medical segmentation tasks. This pioneering technique merges shallow and deep features, improving the accuracy and reliability of the segmentation process. Since then, many works have been taken to enhance UNet’s performance in the segmentation task.

UNet++ [4] ameliorates the performance of UNet by nested skip connections. In addition, SFA [14] proposes the boundary-sensitive loss and additional decoder to encourage the model to focus on the polyp boundary. PraNet [5] utilizes a reverse attention module and parallel partial decoder to enhance the precise boundary separating a polyp from the surrounding mucous membrane. MSNet [6] specifically employs cascaded subtraction operations at multiple levels and stages to capture complementary information from different levels.

Recently, Hieu *et al.* [15], and PEFNet [7] concentrate on the positional information, improving the overall detection of polyp regions. In general, most methods seem to ignore useful information of the decoder’s features. We believe that by capturing the multi-level information of the decoder, the model can achieve more accurate polyp localization.

In summary, UNet and its variants, along with techniques like skip connections, boundary-sensitive loss, attention mechanisms, and positional cues, have significantly advanced polyp segmentation. But there is still potential in harnessing the decoder’s features to further improve accuracy.

III. METHODS

A. General architecture

A novel M²UNet is built by extending the UNet architecture by incorporating modifications inspired by the ConvFormer and Transformer blocks from the MetaFormer baseline in the encoder stage. Additionally, we introduce the utilization of the Multi-scale Upsampling module (MU) to enhance the multi-scale representation of the decoder. The complete architecture is illustrated in Figure 1.

The input tensor $X \in R^{W \times H \times 3}$ has a shape of $W \times H \times 3$, where W represents the width, H represents the height, and the encoder extracts features $X_i \in R^{\frac{W}{2^{i+1}} \times \frac{H}{2^{i+1}} \times F_i}$ at different stages, denoted by $F_i \in \{64, 128, 320, 512\}$ and $i \in \{1, 2, 3, 4\}$, representing the filters used at each step of the encoder and decoder stages.

In the decoder stage, although the feature is upsampled twice using Convolution Transpose 2D at each step, we further enhance the feature by employing our Multi-scale Upsampling block (MU), which upsamples the feature four times at step i . The upsampled features are then merged with the features at step $i - 2$ to enrich the feature representation while incorporating the previously upsampled features.

Following this, the decoder stage generates a mask with a shape of $W \times H \times 64$. Subsequently, a 1×1 Convolution layer is applied to map the feature map from 64 filters to a single filter, producing the final output.

B. ConvFormer Block

In the MetaFormer [8], the ConvFormer block investigates the capabilities of established token mixers to achieve excellent performance. Instead of developing new token mixers, the block relies on commonly-used operators to assess the lower limits of performance and model versatility.

The ConvFormer block consists of four steps. The first step involves creating token mixers. To accomplish this, the Convolution operation is employed using two specific techniques: Depthwise Convolution and Separable Convolution. These convolutional operations are utilized to enhance the mixing of tokens within the model architecture, promoting effective information exchange and integration across different parts of the input sequence.

$$Conv(X_i) = Conv_{pw2}(Conv_{dw}(\sigma(Conv_{pw1}(X_i)))) \quad (1)$$

$$X_i = X_i + Conv(Norm(X_i)) \quad (2)$$

$$Xi = Xi + \sigma(Norm(Xi)W_1)W_2 \quad (3)$$

Equations 1, 2, and 3, referenced in the paper [8], introduce the ConvFormer block. Within this equation, $Conv_{pw}$ represents the pointwise Convolution operation applied at index i , while $Conv_{dw}$ refers to the Depth-wise Convolution operation. In the subsequent stages, the output of equation 1 is normalized before the skip connection is incorporated. Following the normalization step, equation 2 demonstrates the application of the skip connection to the normalized output. Equation 3 also demonstrates the skip connection output is adjustable by utilizing two learnable parameters, denoted as W_1 and W_2 . They are applied in the Channel MLP layer showcasing this adjustment, where W_1 and W_2 are used to modify the output and shape it according to the desired characteristics or patterns. The activation function $\sigma(\cdot)$ is applied to the output of the Channel MLP layer, introducing non-linearity and enhancing the expressive power of the ConvFormer block.

C. Transformer Block

The Transformer block incorporates the fundamental principles of the conventional Transformer. It consists of a traditional self-attention mechanism that generates an attention mask. By utilizing this self-attention mechanism, the model can focus on various segments of the input sequence and comprehend the interrelationships among its features. The attention feature is derived from the resemblance between the input tokens, which determines the significance of each token in the ultimate output. This mechanism facilitates the model in grasping distant connections and contextual details.

$$X_i = X_i + SelfAttention(Norm(X_i)) \quad (4)$$

$$X_i = X_i + \sigma(Norm(X_i)W_1)W_2 \quad (5)$$

In Equation 4, the self-attention mechanism, known as Self Attention, is introduced. This mechanism governs the computation of the output. Equation 5 represents the skip connection that is applied. The resulting output can be adjusted

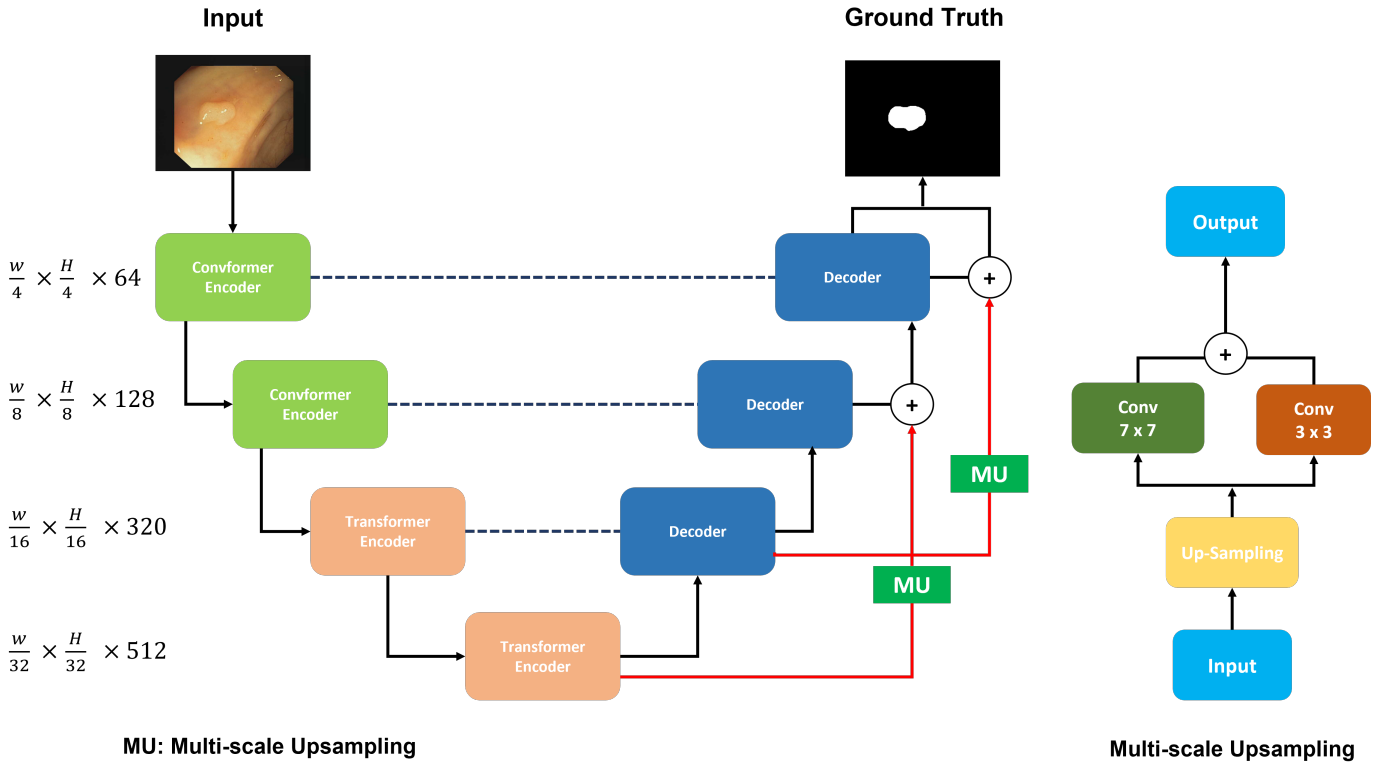


Fig. 1. General architecture of M²UNet

by utilizing two learnable parameters, namely W_1 and W_2 , which originate from the Channel MLP layer.

D. Multi-scale Upsampling Block

The Multi-scale Upsampling block (MU) comprises two stages. The first is the Upsampling stage, where the input data is upsampled to a higher resolution. This process increases the spatial dimensions of the data, while the second stage is the Multi-scale Addition, where multiple scales or resolutions of the upsampled data are added together. This addition operation allows for incorporating information from different scales, enabling the model to capture fine-grained and high-level features. Combining information from multi-scale gives the model a more comprehensive understanding of the polyp foreground and background, thus making more accurate predictions.

$$X_i = \text{Upsampling}(X_i) \quad (6)$$

$$X_i = \text{Conv}_{3 \times 3}(X_i) + \text{Conv}_{7 \times 7}(X_i) \quad (7)$$

$$X_{i-2} = \sigma(X_{i-2} + X_i) \quad (8)$$

Equation 6 describes the Upsampling stage, in which the nearest interpolation is used. The $X_i \in R^{W \times H \times C}$ denotes the input tensor at stage i . Following this, the Multi-scale Addition is performed by extracting the input tensor through two convolution layers with kernel sizes of 3×3 and 7×7 . Two output features are added to create the decoder's output features at stage i , as seen in Equation 7.

Finally, the Multi-scale Upsampling feature is added with the feature output at the decoder stage $i - 2$ to form the new representation feature of the decoder. After that, the activation function $\sigma(\cdot)$ is applied to the output, further enhancing the non-linear mapping and introducing the model's non-linearity; the full equation is described in Equation 8.

IV. EXPERIMENTS

A. Dataset

To conduct the fair comparison, we follow the merged dataset from the PraNet [5] for training which includes 900 samples from Kvasir-SEG [9] and 550 samples from CVC-ClinicDB [10]. The remaining images of Kvasir-SEG [9] and CVC-ClinicDB [10] with three unseen datasets, including ColonDB [11], CVC-300 [13] and ETIS [12] are used for benchmarking.

B. Implementation Details and Evaluation Metrics

All architectures are implemented using the Keras framework with TensorFlow as the backend. Input images are normalized to the range $[-1, 1]$. Adam optimization [16] is utilized with an initial learning rate of $1e-4$. Subsequently, the Cosine Annealing learning rate schedule stabilizes the training process.

The experiments are conducted on a single NVIDIA Tesla A100 40GB GPU with a batch size of 128. Training the entire dataset takes approximately 6 hours. The model is trained for 158 epochs. The images are resized to 352×352 during the

training and inference stages. Augmentation techniques such as Center Crop, Random Rotate, GridDistortion, CutOut [17], CutMix [18], Horizontal and Vertical Flip are applied.

The Jaccard loss function used to supervise our model in the training process can be formulated as follows:

$$JaccardLoss(y, \hat{y}) = \alpha \times \left(1 - \frac{\alpha + \sum_c y_c \times \hat{y}_c}{\alpha + \sum_c y_c + \hat{y}_c - y_c \times \hat{y}_c} \right) \quad (9)$$

The Jaccard Loss, which is shown in Equation 9, is also called the Intersection over Union (IOU) metric [19]. The true label is denoted as y , while the predicted label is represented as \hat{y} . Both labels are expressed as one-hot vectors, indicating the classes with a length equivalent to the number of classes, denoted as C . The α smoothing factor is set to 0.7 in our method. Note that we do not use deep supervision techniques to train our model.

We adopt three evaluation common metrics for quantitative evaluation: mean Dice (mDice), mean IoU (mIoU), and Mean Absolute Error (MAE) to evaluate our method’s performance. The higher value is better for mDice as well as mIoU, and the lower is better for MAE.

C. Performance Comparisons

To evaluate the effectiveness of our model, we compare M²UNet with several methods, including UNet [3], UNet++ [4], SFA [14], PraNet [5], MSNet [6], Hieu *et al.* [15] and PEFNet [7]. Since the setting datasets of Hieu *et al.* [15] and PEFNet [7] are different, we retrain both methods on the same setting in PraNet [5] for a fair comparison.

1) *Quantitative Result:* As shown in Table I, our M²UNet attains superior performance in CVC-300 and ColonDB datasets, demonstrating our model’s ability in the unseen domain. On the other three unseen datasets, *i.e.* Kvasir, ClinicDB, and ETIS, the M²UNet also obtains the second-highest score even though we do not utilize the deep supervision technique.

2) *Qualitative Result:* In Figure 2, we perform the qualitative visualization for several methods. It can be seen that our method can cover more accurate polyp regions. In general, our MU can better highlight the polyp regions based on the multi-scale information of different levels of the decoder.

D. Ablation Study

To evaluate the effectiveness of the MU module, we conduct the ablation study on the Kvasir dataset. As described above, the standard MU module includes two stages, Upsampling and Multi-scale Addition. We analyze the quantitative contribution of both Upsampling stage and MU module to the model performance, which is shown in Table II.

According to the empirical findings, integrating the Metaformer backbone with UNet yields a dice score of 0.874. Including an additional Upsampling stage leads to a gradual improvement in the score, reaching 0.882. Introducing Multi-scale Upsampling further enhances the results slightly, raising the score to 0.891.

	Methods	<i>mIoU</i> ↑	<i>mDice</i> ↑	<i>MAE</i> ↓
Kvasir	UNet [3]	0.756	0.821	0.055
	UNet++ [4]	0.743	0.820	0.048
	SFA [14]	0.611	0.723	0.075
	PraNet [5]	0.840	0.898	0.030
	MSNet [6]	0.862	0.907	<u>0.028</u>
	Hieu <i>et al.</i> [15]	0.835	0.891	0.029
	PEFNet [7]	0.833	0.892	0.029
	M²UNet	<u>0.855</u>	0.907	0.025
ClinicDB	UNet [3]	0.767	0.824	0.019
	UNet++ [4]	0.729	0.794	0.022
	SFA [14]	0.607	0.700	0.042
	PraNet [5]	0.849	0.899	<u>0.009</u>
	MSNet [6]	0.879	0.921	0.008
	Hieu <i>et al.</i> [15]	0.787	0.844	0.019
	PEFNet [7]	0.814	0.866	0.010
	M²UNet	<u>0.853</u>	<u>0.901</u>	0.008
CVC-300	UNet [3]	0.639	0.717	0.022
	UNet++ [4]	0.636	0.687	0.018
	SFA [14]	0.329	0.467	0.065
	PraNet [5]	0.797	0.871	0.010
	MSNet [6]	0.807	0.869	0.010
	Hieu <i>et al.</i> [15]	0.812	0.884	0.006
	PEFNet [7]	0.797	0.871	0.010
	M²UNet	0.819	0.890	<u>0.007</u>
ColonDB	UNet [3]	0.449	0.519	0.061
	UNet++ [4]	0.410	0.483	0.064
	SFA [14]	0.347	0.469	0.094
	PraNet [5]	0.640	0.712	0.043
	MSNet [6]	<u>0.678</u>	<u>0.755</u>	0.041
	Hieu <i>et al.</i> [15]	0.626	0.694	<u>0.037</u>
	PEFNet [7]	0.638	0.710	0.036
	M²UNet	0.684	0.767	0.036
ETIS	UNet [3]	0.343	0.406	0.036
	UNet++ [4]	0.344	0.401	0.035
	SFA [14]	0.217	0.297	0.109
	PraNet [5]	0.567	0.628	0.031
	MSNet [6]	0.664	0.719	<u>0.020</u>
	Hieu <i>et al.</i> [15]	0.589	0.655	0.037
	PEFNet [7]	0.572	0.636	0.019
	M²UNet	<u>0.595</u>	<u>0.670</u>	0.024

TABLE I
QUANTITATIVE RESULTS WITH PREVIOUS METHODS.
THE HIGHEST AND SECOND HIGHEST SCORES ARE SHOWN IN
BOLD AND UNDERLINE, RESPECTIVELY.

By incorporating two Upsampling stages, the dice score improves to 0.899. Notably, when employing the complete pipeline, the score experiences a substantial boost, reaching 0.907.

The ablation study results demonstrate our assumption that capturing multi-level information of multiple decoder stages will ameliorate the model’s ability to identify the polyp objects. By combining the Multi-scale Addition stage of our MU, the model can exploit multi-scale features of shallow stages to complement the necessary information further, thus attaining better performance.

Model	<i>mIoU</i> ↑	<i>mDice</i> ↑	<i>MAE</i> ↓
Baseline	0.819	0.874	0.029
+1 Upsampling	0.827	0.882	0.030
+1 MU	0.833	0.891	0.029
+2 Upsampling	0.843	0.899	0.028
+2 MU	0.855	0.907	0.025

TABLE II
ABLATION STUDY ON THE KVASIR-SEG DATASET [9]

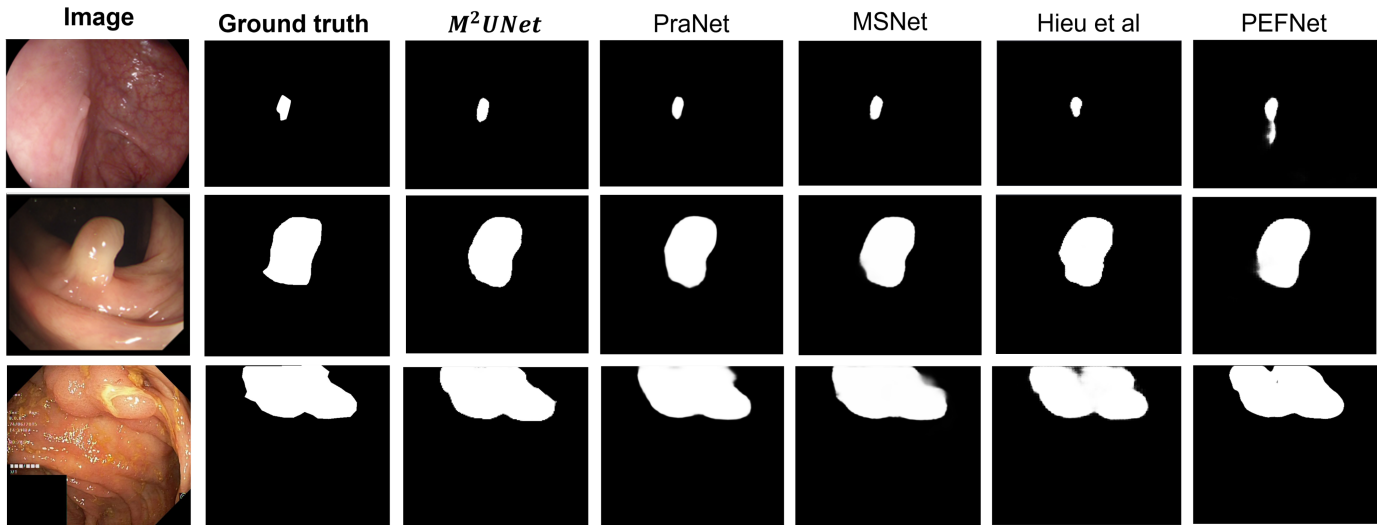


Fig. 2. Qualitative results from various methods

V. CONCLUSION

In this paper, we propose the MetaFormer baseline combined with UNet and our Multi-scale Upsampling block (MU) for the polyp segmentation task. Our M^2UNet is designed to solve the problem from existing methods, which is the locality of the standard convolution operations and the lack of attention to the multi-level information of the decoder’s features.

We believe that capturing multi-scale features of shallow decoder stages and combining them with the higher ones will endow our model to attain more meaningful information about the polyp regions. Extensive experiments and ablation results have demonstrated the improvement of our approach to previous methods.

Although there are some limitations of the M^2UNet that need to be improved, this is a promising method for the polyp segmentation task. Future research should focus on leveraging the full potential of the decoder module for more precise and reliable polyp localization.

ACKNOWLEDGEMENT

This research is funded by Vietnam National University Ho Chi Minh City (VNU-HCM) under grant number DS2020-42-01.

REFERENCES

- [1] M. M. Center, A. Jemal, R. A. Smith, and E. Ward, “Worldwide variations in colorectal cancer,” *CA: a cancer journal for clinicians*, 2009.
- [2] C. Niek van Dijk, G. E. van Dyk, P. E. Scholten, and N. P. Kort, “Endoscopic calceoplasty,” *The American journal of sports medicine*, vol. 29, pp. 185–189, 2001.
- [3] O. Ronneberger, P. Fischer, and T. Brox, “U-Net: Convolutional Networks for Biomedical Image Segmentation,” in *MICCAI*, 2015.
- [4] Z. Zhou, M. M. Rahman Siddiquee, N. Tajbakhsh, and J. Liang, “UNet++: A Nested U-Net Architecture for Medical Image Segmentation,” in *Deep Learning in Medical Image Analysis and Multimodal Learning for Clinical Decision Support*, 2018.

- [5] D.-P. Fan, G.-P. Ji, T. Zhou, G. Chen, H. Fu, J. Shen, and L. Shao, “Pranet: Parallel reverse attention network for polyp segmentation,” in *MICCAI*, 2020.
- [6] X. Zhao, L. Zhang, and H. Lu, “Automatic Polyp Segmentation via Multi-scale Subtraction Network,” in *MICCAI*, 2021.
- [7] T.-H. Nguyen-Mau, Q.-H. Trinh, N.-T. Bui, P.-T. V. Thi, M.-V. Nguyen, X.-N. Cao, M.-T. Tran, and H.-D. Nguyen, “PEFNet: Positional Embedding Feature for Polyp Segmentation,” in *Multimedia Modeling*, 2023.
- [8] W. Yu, M. Luo, P. Zhou, C. Si, Y. Zhou, X. Wang, J. Feng, and S. Yan, “Metaformer is actually what you need for vision,” in *CVPR*, 2022.
- [9] D. Jha, P. H. Smedsrud, M. A. Riegler, P. Halvorsen, T. d. Lange, D. Johansen, and H. D. Johansen, “Kvasir-SEG: A Segmented Polyp Dataset,” in *Multimedia Modeling*, 2020.
- [10] J. Bernal, F. J. Sánchez, G. Fernández-Esparrach, D. Gil, C. Rodríguez, and F. Vilariño, “WM-DOVA maps for accurate polyp highlighting in colonoscopy: Validation vs. saliency maps from physicians,” *CMIG*, pp. 99–111, 2015.
- [11] N. Tajbakhsh, S. R. Gurudu, and J. Liang, “Automated Polyp Detection in Colonoscopy Videos Using Shape and Context Information,” *TMI*, pp. 630–644, 2016.
- [12] J. S. Silva, A. Histace, O. Romain, X. Dray, and B. Granado, “Towards embedded detection of polyps in WCE images for early diagnosis of colorectal cancer,” *IJCARS*, pp. 283–293, 2014.
- [13] D. Vázquez, J. Bernal, F. J. Sánchez, G. Fernández-Esparrach, A. M. López, A. Romero, M. Drozdal, and A. C. Courville, “A Benchmark for Endoluminal Scene Segmentation of Colonoscopy Images,” *Journal of Healthcare Engineering*, 2017.
- [14] Y. Fang, C. Chen, Y. Yuan, and K.-y. Tong, “Selective Feature Aggregation Network with Area-Boundary Constraints for Polyp Segmentation,” in *MICCAI*, 2019.
- [15] T.-H. Nguyen-Mau, Q.-H. Trinh, N.-T. Bui, M.-T. Tran, and H.-D. Nguyen, “Multi Kernel Positional Embedding ConvNeXt for Polyp Segmentation,” in *RIVF*, 2022.
- [16] D. P. Kingma and J. Ba, “Adam: A method for stochastic optimization,” *arXiv preprint arXiv:1412.6980*, 2014.
- [17] T. DeVries and G. W. Taylor, “Improved regularization of convolutional neural networks with cutout,” *arXiv preprint arXiv:1708.04552*, 2017.
- [18] S. Yun, D. Han, S. Chun, S. Oh, Y. Yoo, and J. Choe, “CutMix: Regularization Strategy to Train Strong Classifiers With Localizable Features,” in *ICCV*, 2019.
- [19] J. Bertels, T. Eelbode, M. Berman, D. Vandermeulen, F. Maes, R. Bisschops, and M. B. Blaschko, “Optimizing the dice score and jaccard index for medical image segmentation: Theory and practice,” in *MICCAI*, 2019.